Pergamon

0956-7151(94)E0161-9

Acta metall. mater. Vol. 42, No. 11, pp. 3785–3800, 1994
Copyright © 1994 Elsevier Science Ltd
Printed in Great Britain. All rights reserved
0956-7151/94 $7.00 + 0.00

INTERNAL FRICTION IN F.C.C. ALLOYS DUE TO SOLUTE DRAG ON DISLOCATIONS—I. A MODEL FOR THE EFFECT OF CORE DIFFUSION

A. PICHLER† and E. ARZT

Max-Planck-Institut für Metallforschung and Institut für Metallkunde der Universität Stuttgart, D-70174 Stuttgart, Germany

(Received 16 July 1993; in revised form 23 February 1994)

Abstract—The internal friction (mechanical loss) behavior of dislocations is studied in a model which, for the first time, considers the substitutional solute mobility in the dislocation core to be higher than in the bulk around it. The parameters investigated include the external stress σ_{xy}, the solute concentration c_0, the pinning length of the dislocation and the temperature. It is shown that, at low c_0 and high σ_{xy}, the kinetics of the dislocation motion is determined by the fast diffusion of the solute atoms in the core, while for high c_0 and low σ_{xy} the diffusion of the atoms far away from the dislocation is rate-limiting. The results are compared with the analytical model of Schoeck and are applied to the alloy system Al–Si. New experimental results supporting the model are described in a companion paper (Part II).

1. INTRODUCTION

Dislocations are of great importance in the interpretation of many internal friction (mechanical loss) experiments. The kinetics of the dislocation movement may be controlled by different mechanisms [1–4]. Generally, intrinsic dislocation mechanisms, such as the non-conservative movement of jogs on screw dislocations [5], can be distinguished from extrinsic mechanisms, which involve the interaction with other defects, such as solute atoms [6–8]. For describing the movement of a dislocation in internal friction experiments two different model levels are common: The first is based on the Koehler–Granato–Lücke [9, 10] string model, which considers only the line tension and the stress field of a dislocation. On the other level, also the atomistic structure, the periodicity of the lattice and the Peierls potential are taken into account [2]. In materials which are not very pure the following effects can occur:

(i) breakaway from the solute atom cloud [8, 11, 12];
(ii) concurrent motion of dislocation and solute atom cloud [2, 6, 13].

Which case dominates is determined by material parameters (e.g. solute atom concentration) and the testing parameters external stress and temperature.

In this paper only the parameter range in which the dislocation cannot move without the solute atoms is investigated. For this case, longitudinal movement of the solute, i.e. along the dislocation, and transverse movement, i.e. normal to the dislocation, are considered [13, 14]. The motivation for this study originated in some internal friction results for Al–Si single crystals [15, 16], where a loss maximum was obtained which was caused by dislocations but had a lower activation enthalpy than that for volume diffusion. As longitudinal movement and breakaway from the solute cloud could be excluded, this behavior was in principle explained by a transverse movement of the solute atoms and by the main assumption of a higher mobility (lower activation enthalpy) for solute diffusion in the dislocation core. It remained unclear however under which conditions these solute atoms in the core region determine the activation enthalpy of the internal friction process.

While a higher *longitudinal* mobility of the solute in the dislocation core is well established for internal friction [4, 13, 17], the possibility of a lower activation enthalpy for *transverse* diffusion in the dislocation core has not been considered in the literature up to now. The following numerical model studies the consequences of such an effect as a function of the parameters external shear stress σ_{xy}, solute atom concentration c_0, length l of the dislocation between the pinning points and temperature T. The calculations are conducted for the quasi-static case, in which a constant stress σ_{xy} acts on the dislocation. The bowing of the dislocation and the resulting anelastic strain are computed as a function of time. From this response function, the strain as a function of time and the relaxation parameter for dynamic internal friction are deduced. The symbols used are listed in the Nomenclature at the end.

†Present address: VOEST ALPINE Stahl Linz GmbH, Linz, Austria.

2. THE MODEL

2.1. Assumptions and approximations

Consider an edge dislocation in a material, pinned at distances l by dislocation nodes or particles and surrounded by a Cottrell cloud of substitutional solute atoms. An external stress now attempts to bow out the dislocation between the pinning points. Only the case in which the concurrent movement of the Cottrell cloud determines the kinetics is considered. Dislocation movement stops once the force on the dislocation is balanced by the line tension.

In order to arrive at a tractable model the following approximations are made:

(i) The dislocation is treated as a flexible string [3, 18]. This is admissible if the deviation between the Peierls valley and the dislocation line is large enough (for f.c.c. metals larger than $\sim 4°$ [1]) for the kinks to overlap. The line tension T_L is given to a reasonable approximation by $Gb^2/2$, where G is the shear modulus and b the Burgers vector. The discrete nature of the lattice and of the Peierls relief are not considered. Therefore a contribution from the kink pair generation to the activation energy (~ 0.1 eV for Al) is neglected for dislocations parallel to the Peierls valley; this important local mechanism should not greatly influence the overall behavior of the solute cloud.

(ii) The dislocation field is described by the elastic field of a Peierls–Nabarro-dislocation [19], an assumption which avoids the stress singularity at the dislocation core.

(iii) During bowing of the dislocation, the elements ds along the line (Fig. 1) have different velocities. To circumvent a time-consuming three-dimensional problem, a rigid dislocation with a constant velocity is assumed. The influence of the bowing-out is simulated by subtracting from the external stress a back stress of the following form (for derivation see Appendix A1)

$$\sigma_L = 4\frac{Gb}{l^2}x_d \qquad (1)$$

where x_d is the bowing-out distance of the dislocation between the pinning points.

(iv) The distribution of the solute atoms around the dislocation is described by a concentration field $c = c(x, y)$. This function can be interpreted as the probability of finding a solute atom in an infinitesimal volume element. The movement and the effects of single atoms are not considered in the model.

(v) The field around the dislocation is divided into two regions (Fig. 2): core diffusion is assumed to dominate in a square interior region with an edge length of $2b$ ("core region"), outside this region only bulk diffusion operates ("bulk region"). Diffusion of the solute atoms is described by a jump rate equation.

2.2. Model calculations

The calculation procedure can be summarized as follows. First, a finite-difference mesh is constructed around the dislocation as shown in Fig. 2. (The nodes of this mesh are of course *not* atomic positions.) Then the equilibrium distribution of a given concentration of solute atoms in the vicinity of the dislocation is calculated and the corresponding values are allocated to the nodes. At time $t = 0$ an external stress is applied, which bows the dislocation until the forces due to external stress, line tension and solute atoms balance to zero. Next the solute cloud, which is now not in equilibrium with the dislocation, has to be adjusted: in a time step Δt the solute atoms move by diffusion toward a new equilibrium distribution. After this diffusion step the force exerted on the dislocation by the solute atoms is lower and the dislocation can bow further. By a combination of these two steps the bowing of the dislocation is calculated as a function of time. The dislocation motion finally stops when the force due to the line tension is equal to the force due to the external stress; the solute atoms, now in equilibrium, do no longer exert any stress.

For the initial solute distribution around the straight dislocation an ideal segregation obeying the Fermi–Dirac distribution [20] is assumed

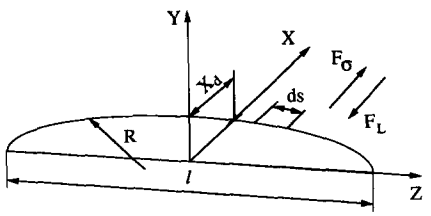

Fig. 1. Configuration for describing the movement of a pinned edge dislocation under an external stress σ_{xy}. F_σ denotes the force due to the external stress and F_L the force due to the back stress arising from the line tension.

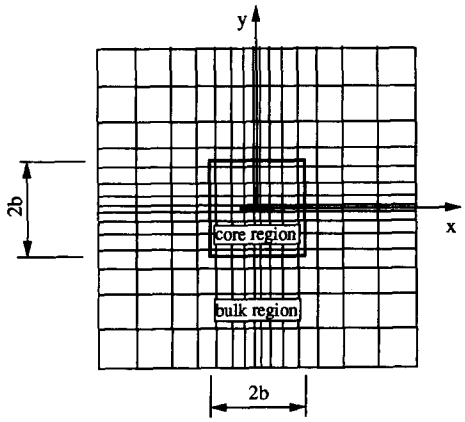

Fig. 2. Schematic of the mesh for solving the diffusion problem and for calculating the forces exerted on the dislocation by the solute atoms. For the core and bulk regions different solute diffusivities are assumed.

$$c(x,y)=\frac{1}{1-\dfrac{1-c_0}{c_0}\cdot\exp(E/kT)} \tag{2}$$

where c_0 is the number concentration far away from the dislocation, E the interaction energy between dislocation and solute atom, k Boltzmann's constant, and T the absolute temperature.

For this interaction energy the elastic solution for a misfitting sphere is used [21]

$$E=A\frac{y\pm\xi}{(x-x_d)^2+(y\pm\xi)^2} \tag{3}$$

where

$$A=\frac{1+\nu}{1-\nu}\cdot\frac{G\cdot b}{\pi}\cdot\epsilon\cdot\Omega$$

and Ω is the atomic volume of the matrix, ϵ the elastic misfit of a solute atom, ν Poisson's ratio, and ξ the dislocation half width. In equation (3) the $+$ sign is used for $y\geqslant 0$ and the $-$ sign for $y<0$. A computation for Si in Al with the material parameters in Table 1 gives the realistic energy of 0.23 eV for the interaction between a solute atom in the dislocation core and the dislocation.

The force exerted by a misfitting solute atom at x, y on a dislocation bowed out to x_d is calculated according to

$$F=-\frac{\partial E}{\partial x_d}=2A\cdot\frac{(x_d-x)\cdot(y\pm\xi)}{[(x-x_d)^2+(y\pm\xi)^2]^2}. \tag{4}$$

For computing the force due to the whole Cottrell cloud, equation (4) is multiplied by the probability c of finding a solute atom at x, y in the volume dV and integrated over the volume. Because of the straight dislocation assumption we integrate over the plane x, y to get the force per unit length along z

$$F_S=2A\int_{-\infty}^{+\infty}\int_{-\infty}^{+\infty}\frac{(x_d-x)\cdot(y\pm\xi)}{[(x-x_d)^2+(y\pm\xi)^2]^2}\times\frac{c(x,y)}{\Omega}\cdot dx\cdot dy. \tag{5}$$

For computing the force it is immaterial whether the dislocation moves by x_d in the Cottrell cloud or the Cottrell cloud moves by x_d in the opposite direction. For computational simplicity, the dislocation position is fixed and the solute cloud is moved.

Finally, to readjust the Cottrell cloud, a jump rate equation of the following form must be solved [22, 23]

Table 1. Material parameters used in the calculations, with references

$\epsilon_{\text{Si in Al}}$	-0.045	[25]
b (nm)	0.286	[21]
ξ (nm)	0.1	[21]
G (GPa)	26.5	[21]
ν	0.347	[21]
Ω (m^3)	1.66×10^{-29}	[21]
D_B (m$^2\cdot$s^{-1})	$1.7\times10^{-4}\cdot\exp(-142{,}000/RT)$	[26]
D_C (m$^2\cdot$s^{-1})	$1.7\times10^{-4}\cdot\exp(-82{,}000/RT)$	[26]

$$\frac{\Delta c_{i,j}}{\Delta t}=\frac{D}{h^2}\cdot\left[c_{i,j}(1-c_{i,j-1})\cdot\exp\left(\frac{E_{i,j}-E_{i,j-1}}{2kT}\right)-c_{i,j-1}(1-c_{i,j})\cdot\exp\left(\frac{E_{i,j-1}-E_{i,j}}{2kT}\right)+\cdots\right] \tag{6}$$

where $c_{i,j}$ is the concentration at node (i,j), $E_{i,j}$ the potential energy and $\Delta c_{i,j}/\Delta t$ the change in concentration in a time step, and h is the distance between adjacent nodes. The appropriate diffusion coefficient D is selected by insertion of the corresponding value of Q.

After each diffusion step a new equilibrium position x_d, at which the sum of the forces $F_S+F_\sigma-F_L$ is zero, has to calculated, where $F_\sigma=\sigma_{xy}\cdot b$ is the external force per unit length. Therefore the implicit equation

$$\sigma_{xy}\cdot b-4\cdot\frac{G\cdot b^2}{l^2}\cdot x_d+2A\int_{-\infty}^{+\infty}\int_{-\infty}^{+\infty}\times\frac{(x_d-x)\cdot(y\pm\xi)}{[(x-x_d)^2+(y\pm\xi)^2]^2}\cdot\frac{c(x,y)}{\Omega}\cdot dx\cdot dy=0 \tag{7}$$

has to be solved. The equilibrium value x_d is calculated by regula falsi. To get a sufficiently exact solution for equations (6) and (7), a finer mesh is chosen in the core region than in the bulk region; this is achieved by transforming the problem to a u, v space according to James and Barnett [24].

In order to extract relaxation times τ and relaxation strengths Δ from the calculated data, the bowing-out distance as a function of time is fitted by

$$x_d=\bar{x}_d\cdot[1-\exp(-t/\tau)] \tag{8}$$

where $\bar{x}_d$ is the saturation value of the bowing-out distance. As will be seen, the bowing-out distance often saturates below the maximum possible value because of the line tension. It is therefore useful to define a normalized relaxation strength

$$\Delta=\frac{\bar{x}_d}{x_{d,\max}} \tag{9}$$

where $x_{d,\max}$ is the maximum bowing-out distance limited by the line tension.

3. RESULTS

In this paper all relaxations were calculated for Si solute atoms in an Al matrix (see data in Table 1). As diffusion constants for Si in Al, especially for diffusion in the core, are not known, the values for Al selfdiffusion were used. The "standard parameters", which were selected for all calculations (unless stated otherwise), were $T=400$ K, $l=500$ nm, and $\sigma_{xy}=10^{-5}\cdot G$.

3.1. A computing example and its evaluation

In the following example the consequences of assuming regions with different diffusivities are demonstrated. The calculation was executed for

$c_0 = 6 \times 10^{-5}$. To avoid instabilities in the numerical solution of equation (6) the time steps Δt were adapted to the faster core diffusion process ($\Delta t = \Delta t_C = 5 \times 10^{-9}$ s).

Figure 3 shows the bowing-out distance x_d calculated in this way as a function of time. After a fast initial movement the dislocation slows down and x_d converges to a saturation value. This final limit is determined by the driving force ($F_\sigma - F_L$) and the force exerted by the "bulk solute" (i.e. solute atoms in the bulk region), which has not moved in the short time step. By comparison, the "core solute" (i.e. solute atoms in the core region) has moved with the dislocation and exerts only a negligible force. For simplicity, we will denote this regime of relaxation due to diffusion of solute in the core region as "core relaxation".

The balance of forces is illustrated in Fig. 4: the force F_σ due to the external stress is constant, while the net driving force $F_\sigma - F_L$ decreases linearly with increasing bowing-out distance. The back-driving force, which is exerted by the "bulk solute", is shown as the curved line ($F_{S,B}$); after going through a maximum, $F_{S,B}$ approaches the driving force such that the velocity converges to zero and the bowing-out distance reaches a saturation value, as seen in Fig. 3. Because of the asymptotic behavior, the calculation was stopped at

$$0.975 \cdot F_\sigma - F_L + F_{S,B} < 0. \qquad (10)$$

This corresponds to the end points marked in Figs 3 and 4.

As the bowing-out due to "core relaxation" saturates, further dislcoation motion requires diffusion of the "bulk solute". In this regime of "bulk relaxation" the time steps Δt_B were chosen to be larger by about a factor of 10^6 ($= D_B/D_C$) than Δt_C. To avoid instabilities in the core region the fact was used that after the first part of the calculation the solute atom distribution in the core region is nearly in equilibrium. Therefore, in the following calculation the

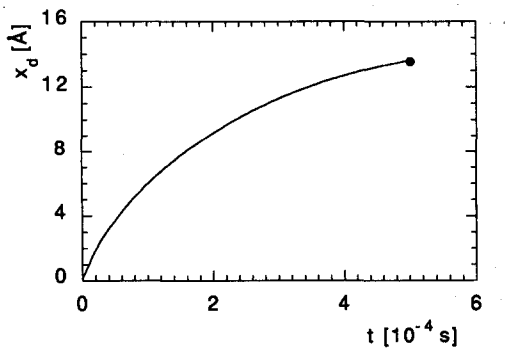

Fig. 3. The first stage of the bowing-out ($x_{d,c}$) of a dislocation as a function of time. The kinetics of the movement is determined by fast diffusion of the "core solute". The calculation is interrupted at the end point of the curve.

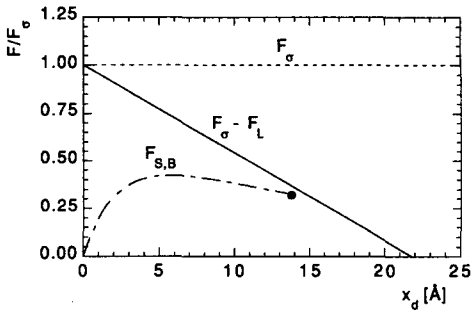

Fig. 4. The forces acting on the dislocation during the movement shown in Fig. 3 as a function of the bowing-out distance. The velocity in Fig. 3 falls as the net driving force ($F_\sigma - F_L$) approaches the back-driving force due to the "bulk solute" ($F_{S,B}$). The bowing-out distance is determined by the force of the "bulk solute", which does not move within the time steps characteristic for diffusion in the dislocation core.

solute atom distribution in the core region was taken into equilibrium, without diffusion steps following equation (6) [15].

From these results the following conclusion concerning the role of the two solute regions, as shown schematically in Fig. 5, can be drawn: the *kinetics* of the first step (the "core relaxation regime") is controlled by the "*core solute*" [Fig. 5(a–c)]. However the maximum bowing-out distance, which is proportional to the *relaxation strength*, is determined by the "*bulk solute*". In the second step (the "bulk relaxation regime"), both the *kinetics* and the *relaxation strength* are determined by the diffusion of the "*bulk solute*" [Fig. 5(d, e)]. From the bowing-out distance in the "core and bulk relaxation" regimes as a function of time, the relaxation times and normalized strengths were calculated according to equations (8) and (9).

3.2. *The shape of the Cottrell cloud*

The shape of the Cottrell cloud, which is shown schematically in Fig. 5, was now calculated in the regimes of "core relaxation" and of "bulk relaxation". In the former case, $\sigma_{xy} = 10^{-5} \cdot G$, $c_0 = 3 \times 10^{-5}$, $l = 500$ nm, and $T = 400$ K were chosen. The resulting Cottrell clouds for $x_{d,C} = 0$, 3 and 11 Å are shown in Fig. 6(a–c), where the concentrations are plotted in the transformed u, v space. The bowing-out of the dislocation as a function of the time is plotted in Fig. 6(d). Figure 6(a–c) correspond to the schematic sketch in Fig. 5(a–c). The first plot [Figs 6(a) and 5(a)] shows the symmetric equilibrium distribution at the beginning. At an intermediate stage [Figs 6(b) and 5(b)] the distributions of the "core solute" and of the "bulk solute" have become asymmetric. The strong forces from the "core solute" are reflected in the asymmetry of the Cottrell cloud near the dislocation. In the third plot [Figs 6(c) and 5(c)] the asymmetry of the core region has decreased, while the bulk region is heavily distorted. The conse-

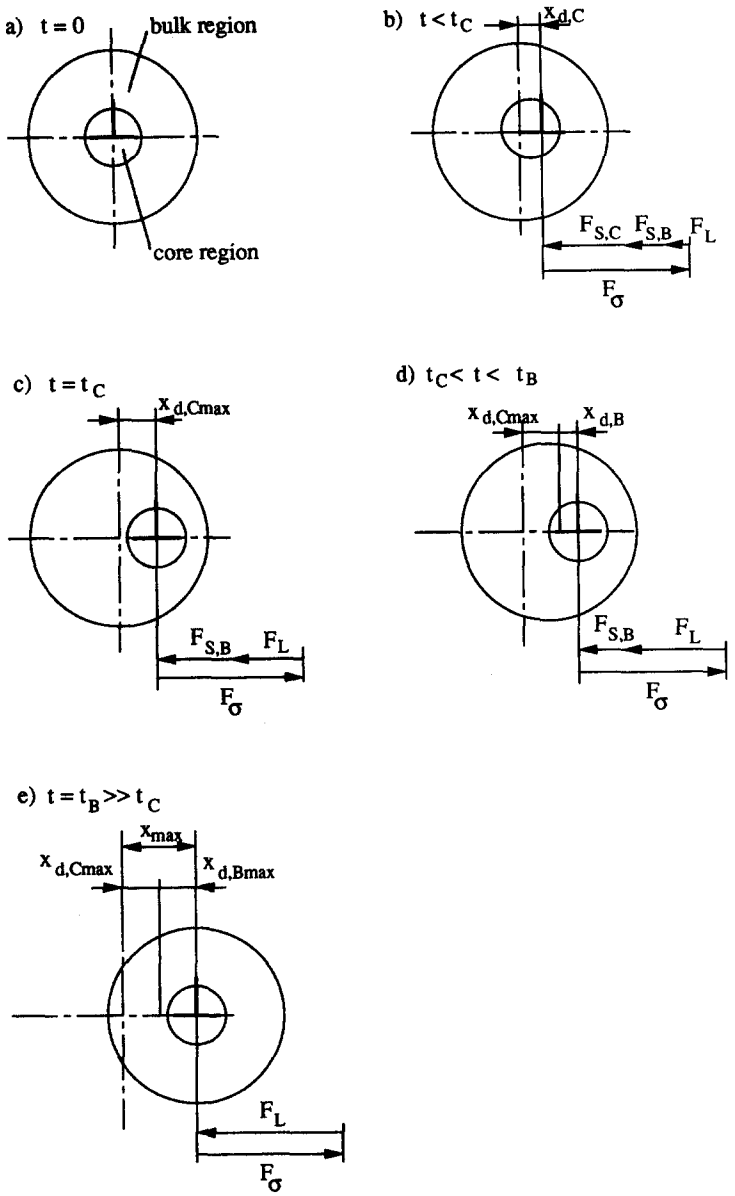

Fig. 5. Schematic of the sequence of events treated in the model: the shape of the Cottrell cloud in the core region (=small circle) and the bulk region (=large circle) is indicated for five different bowing-out distances. The forces on the dislocation (as in Fig. 4) are depicted for each stage, where F_σ is the force due to the external stress, F_L the back driving force due to the line tension, $F_{S,B}$ the force exerted by the "bulk solute", and $F_{S,C}$ the force exerted by the "core solute". (a) Initial configuration: The solute clouds within the core and bulk region are symmetric. (b) Intermediate stage for "core relaxation": The "core solute" diffuses with the dislocation in contrast to the "bulk solute" which does not. The action of the forces $F_{S,B}$ and $F_{S,C}$ which balance the net driving force $(F_\sigma - F_L)$ is reflected in the asymmetry of the solute cloud. (c) "End point" configuration for the "core relaxation" and start configuration for the "bulk relaxation": at the end of the core relaxation the "core solute" distribution is nearly in equilibrium and the net driving force is balanced by the bulk solute. (d) Intermediate stage for "bulk relaxation": The "core solute" is in equilibrium while the bulk solute is still asymmetrically distributed. The external force is balanced by the force exerted by the bulk solute and the line tension. (e) "End-point" configuration for the "bulk relaxation": The solute distributions of the "core" and "bulk solute" are now in equilibrium. The external force is balanced only by the line tension.

quence is a lower force of the "core solute" and a higher force of the "bulk solute" acting on the dislocation.

For calculating the solute distribution during "*bulk* relaxation", a higher solute concentration $c_0 = 3 \times 10^{-4}$ was chosen. As a starting configuration, the "end-point" situation of the "core relaxation" was assumed. The evolution of the solute distribution in Fig. 7(a–c) can be compared with the schematic in Fig. 5(c–e). It is seen that the asymmetry of

the Cottrell cloud, and therefore the force $F_{S,B}$, decreases during the bowing-out. At the end of the calculation the solute distribution is nearly in equilibrium and the external force is balanced only by the line tension. The generally less-pronounced asymmetry in Fig. 7(a–c) when compared to Fig. 6(a–c) is due to the higher solute concentration.

3.3. The influence of the parameters σ_{xy}, c_0, l and T
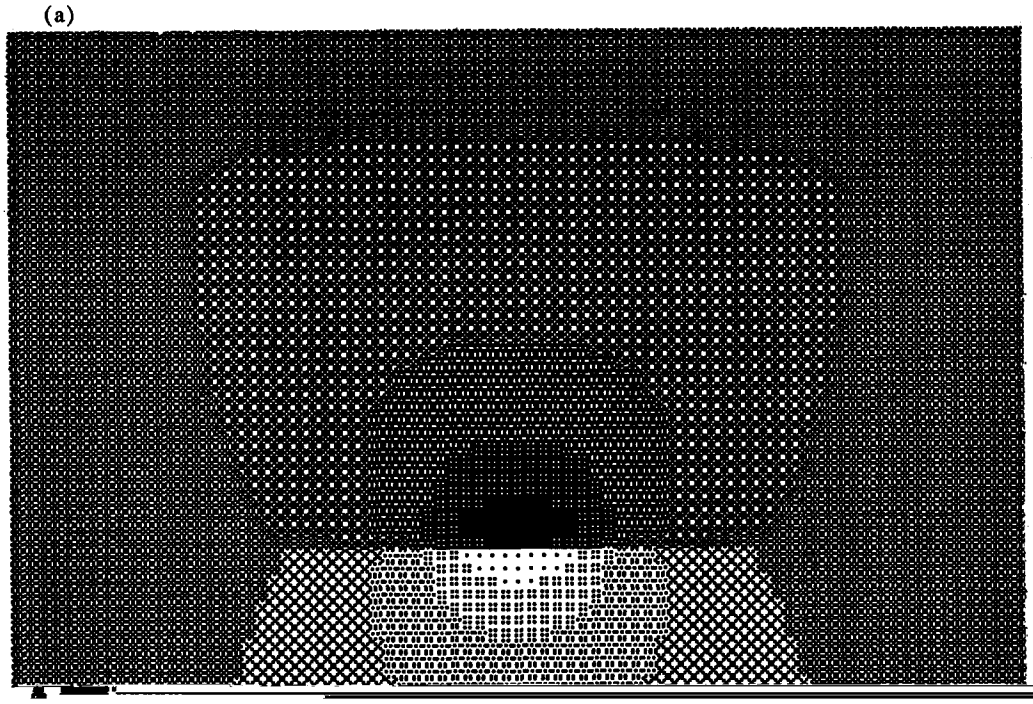
To study the effect of the solute concentration and of the external stress, parameters for which the dominating mechanism changes from "core" to "bulk relaxation" were selected. For studying the influence of l and T, parameters were used for which one mechanism clearly dominates.